PNAS 118.9 (2021): e2015285118

DOI: https://doi.org/10.1073/pnas.2015285118

Primitive Selection of the Fittest Emerging through Functional Synergy in Nucleopeptide Networks

Anil Kumar Bandela,[a] Nathaniel Wagner,[a] Hava Sadihov,[a] Sara Morales-Reina,[b] Agata Chotera-Ouda,[a,c] Kingshuk Basu,[a] Rivka Cohen-Luria,[a] Andrés de la Escosura[b,d]* and Gonen Ashkenasy[a]*

[a] Department of Chemistry, Ben-Gurion University of the Negev, Beer-Sheva 84105, Israel.

[b] Department of Organic Chemistry, Universidad Autónoma de Madrid, Campus de Cantoblanco, 28049 Madrid, Spain.

[c] Current address: Centre of Molecular and Macromolecular Studies, Polish Academy of Sciences, Sienkiewicza 112, 90-363 Lodz, Poland.

[d] Institute for Advanced Research in Chemistry (IAdChem), Cantoblanco, 28049 Madrid, Spain.

* Corresponding author emails: A.d.l.E: andres.delaescosura@uam.es.; G.A.: gonenash@bgu.ac.il

Abstract

Many fundamental cellular and viral functions, including replication and translation, involve complex ensembles hosting synergistic activity between nucleic acids and proteins/peptides. There is ample evidence indicating that the chemical precursors of both nucleic acids and peptides could be efficiently formed in the prebiotic environment. Yet, studies on non-enzymatic replication, a central mechanism driving early chemical evolution, have focused largely on the activity of each class of these molecules separately. We show here that short nucleopeptide chimeras can replicate through autocatalytic and cross-catalytic processes, governed synergistically by the hybridization of the nucleobase motifs and the assembly propensity of the peptide segments. Unequal assembly-dependent replication induces clear selectivity towards the formation of a certain species within small networks of complementary nucleopeptides. The selectivity pattern may be influenced and indeed maximized to the point of almost extinction of the weakest replicator, when the system is studied far from equilibrium and manipulated through changes in the physical (flow) and chemical (template and inhibition) conditions. We postulate that similar processes may have led to the emergence of the first functional nucleic-acid–peptide assemblies prior to the origin of life. Furthermore, spontaneous formation of related replicating complexes could potentially mark the initiation point for information transfer and rapid progression in complexity within primitive environments, which would have facilitated the development of a variety of functions found in extant biological assemblies.

The rich, highly efficient and specific biochemistry in living cells is orchestrated by molecules belonging to a small number of families, primarily nucleic acids, proteins, fatty acids, and sugars. Many fundamental cellular and viral functions, including replication and translation, are facilitated by synergistic activity in complexes of these molecules, very often involving nucleic acids (DNA, RNA or their constituent nucleotides/nucleobases) and proteins (or peptides/amino acids). Among the most important examples of such complexes are the nucleosome, which comprises DNA packaging units in eukaryotes, the ribosome, which translates RNA sequences into proteins, and amino-acid-charged *t*-RNA conjugates, which are exploited during translation.[1-4] In order to harness such synergistic activity in synthetic materials, several groups (including the authors) have recently studied the co-assembly of nucleic acids with (often) positively charged peptides or the self-assembly of premade nucleic-acid–peptide (NA–pep) chimeras.[5-12] It is expected that such assemblies could produce new materials for various applications, such as (auto)catalysis, electron transfer, tissue scaffolding and (drug) delivery.[13-17] Intriguingly, the NA–pep assemblies combine 'digital' molecular information for the hybridization of nucleic acids with 'analog' instructions that affect peptide aggregation and, as such, are expected to show superior behavior in comparison with related nucleic-acid-only or peptide-only assemblies.[18-20]

We now propose that alongside the development of NA–pep conjugate assemblies for new materials, an analysis of the formation of chimeras within complex mixtures, and particularly the selection of specific sequences through replication processes, will offer new insight into their emergence in the early chemical evolution. Indeed, several studies have indicated that evolution in prebiotic environments, towards the origin of life, must have involved cooperative interactions among diverse classes of molecule.[21-24] Other studies, including the seminal works of Eigen[25] and Kauffman[26], have revealed the possible emergence of synergistic activity in prebiotic autocatalytic networks and, as a consequence, phase transitions towards beneficial cooperative and/or selective behavior.[27,28] Importantly, while it has been shown that highly complex functions emerge by wiring together multiple pathways – driving, for example, elaborate feedback loops – our studies, as well as others, have indicated that multiple unique dynamic features,[29-35] including chemical computation,[36] can be developed in relatively small networks.

Despite strong evidence for prebiotic pathways that yield nucleobases and peptides – suggesting that molecules of both families were indeed present in early chemical evolution – prebiotic chemistry research has focused largely on studying each class of molecule separately.[37] This approach has led to incomplete discussions on the 'RNA World', the 'Peptide World' or the 'Metabolism-First World', with minimal overlap between the different domains. In particular, studies on replicating molecules and replication networks have investigated discrete systems affected only by a single class of molecule—whether nucleic acids, peptides, lipid amphiphiles, or small organic molecules.[38-40] Herein, we propose to blur the limits between families of replicators by combining nucleic-acid molecular genetic information with peptide-based assembly 'phenotypes'. To this end, we sought to reveal the self-organization and selection processes taking place in mixtures containing short complementary

nucleopeptide conjugates (designated $\mathbf{R}^{\mathbf{AA}}$ and $\mathbf{R}^{\mathbf{TT}}$; see Fig. 1). Experimental and simulation analyses of the template-directed replication processes within these networks clearly demonstrate that product formation is governed both by nucleobase hybridization and by the formation of unique supramolecular architectures by each of the nucleopeptide conjugates. Unequal assembly-dependent replication capacity induces selectivity towards the formation of $\mathbf{R}^{\mathbf{AA}}$. By studying the system in a flow reactor, namely, at far-from-equilibrium conditions, we show how this selectivity can be influenced and maximized – through changes in the physical (flow) and chemical (template and inhibition) conditions – to the point of almost complete extinction of $\mathbf{R}^{\mathbf{TT}}$, the weaker replicator. We suggest that, prior to the origin of life, processes such as these may have led to the emergence of simple functional NA–pep assemblies,[41] which could facilitate further structural development into the current cellular NA–pep assemblies.

Results and discussion

In non-enzymatic replication, the replicating molecules serve as both templates and catalysts. These replicators either enhance synthesis of their own copies (i.e., self-replication) or participate in reciprocal cross-catalytic cycles with molecules containing complementary structures.[38,39,42,43] The most recent studies have focused on harnessing non-linear replication processes to control information transfer in synthetic networks incorporating multiple reaction pathways and thereby to induce selective product distribution.[44-47] Both the replicators studied here, namely, $\mathbf{R}^{\mathbf{AA}}$ and $\mathbf{R}^{\mathbf{TT}}$, are readily produced by native chemical ligation (NCL)[21] of the respective di-nucleobase thioester electrophile, $\mathbf{E}^{\mathbf{AA}}$ or $\mathbf{E}^{\mathbf{TT}}$, with a Cys-containing nucleophilic peptide **N** (Fig. 1a,b). These replicators and precursor molecules were synthesized in-house and characterized by NMR, HPLC and MS (see Supplementary methods S2 and Figs. s1-s16).

We started our investigation of $\mathbf{R}^{\mathbf{AA}}$ and $\mathbf{R}^{\mathbf{TT}}$ by analyzing their formation in template-free (background) reactions and their replication capacity through either autocatalysis (which is enhanced by seeding at initiation with the respective product as the template) or cross-catalysis (which is enhanced by seeding with the complementary replicator) (Fig. 1a,b). The background reactions started slowly, but after a lag phase they progressed at higher rates, revealing a clear signature of autocatalysis (Fig. 1a,b - *insets*). The rates of the template-seeded reactions were higher than the background reactions, and the replication of both $\mathbf{R}^{\mathbf{AA}}$ and $\mathbf{R}^{\mathbf{TT}}$ via cross-catalysis pathways was more efficient than that via autocatalysis pathways, unprecedentedly indicating the significance of complementary (T-A) hybridization for templating nucleopeptide conjugate replication. For $\mathbf{R}^{\mathbf{AA}}$ formation, the initial rate enhancement via cross-catalysis with $\mathbf{R}^{\mathbf{TT}}$ (60 μM) was about 125%, which is ~4 times higher than the rate enhancement observed for its formation via autocatalysis (Fig. 1a - *inset*). Similarly, the rate enhancement of $\mathbf{R}^{\mathbf{TT}}$ formation via cross-catalysis with $\mathbf{R}^{\mathbf{AA}}$ (60 μM) was close to 190%, i.e., ~3 times higher than that for $\mathbf{R}^{\mathbf{TT}}$ formation via autocatalysis (Fig. 1b - *inset*). As anticipated for template-assisted

reactions, the rate enhancement increased with an increase in the amount of seeded catalyst. Remarkably, the autocatalytic ligation reaction that forms the (potential) replicator containing single adenine and single thymine bases, $\mathbf{R}^{\mathbf{AT}}$, was not enhanced versus the respective background reaction (Fig. s19, Supplementary Schemes and Figures), empirically signifying the utility of the homo-dinucleobase motif as a minimal unit for recognition and replication. This finding might explain the lack of sequence specificity recently observed for the replication of conjugates containing a peptide attached to single nucleobase units.[48] Since in that study the interactions between nucleobases did not play a role in the assembly and replication steps, the authors proposed that simple fibrous assemblies might also drive systems in which information transfer occurs through base-pairing interactions.

To search for systemic emergent behavior,[49] we then studied the binary network formed by $\mathbf{R}^{\mathbf{AA}}$ and $\mathbf{R}^{\mathbf{TT}}$ by monitoring their simultaneous production in template-free and template-seeded reaction mixtures containing $\mathbf{E}^{\mathbf{AA}}$, $\mathbf{E}^{\mathbf{TT}}$, and a stoichiometric amount of **N** (Fig. 1c,d and Fig. s20). In the template-free reaction, the two replicators were formed at similar rates in the early stages, but in the later stages a moderately larger amount of $\mathbf{R}^{\mathbf{AA}}$ versus $\mathbf{R}^{\mathbf{TT}}$ was produced (Fig. s20f), indicating enrichment of the former via catalytic processes involving the newly formed product/template molecules. Significantly, despite the faster production of both $\mathbf{R}^{\mathbf{TT}}$ and $\mathbf{R}^{\mathbf{AA}}$ via cross-catalysis in their separate reaction mixtures (Fig. 1a,b), seeding with either $\mathbf{R}^{\mathbf{TT}}$ or $\mathbf{R}^{\mathbf{AA}}$ resulted in a clear selectivity towards enhanced production of $\mathbf{R}^{\mathbf{AA}}$ (Fig. 1c,d). After 4 h of the (60 μM) $\mathbf{R}^{\mathbf{TT}}$-seeded reaction, $\mathbf{R}^{\mathbf{AA}}$ formation was ~150% higher than $\mathbf{R}^{\mathbf{TT}}$ formation, whereas after 4 h in the (60 μM) $\mathbf{R}^{\mathbf{AA}}$-seeded reaction, formation of $\mathbf{R}^{\mathbf{AA}}$ was ~50% higher than that of $\mathbf{R}^{\mathbf{TT}}$. The preference for $\mathbf{R}^{\mathbf{AA}}$ formation in both the autocatalysis and cross-catalysis reaction pathways was found to be concentration dependent, as shown by the higher rate enhancement observed for reactions seeded with 60 μM versus 20 μM of the templates. The enhanced production of $\mathbf{R}^{\mathbf{AA}}$ reflects asymmetry in the binary network, which could originate from the propensity of $\mathbf{R}^{\mathbf{AA}}$ and $\mathbf{R}^{\mathbf{TT}}$ to assemble into distinctly different supramolecular architectures (see below; Fig. 2); this propensity, in turn, confers dissimilar templating capacities towards condensation of the respective building blocks.

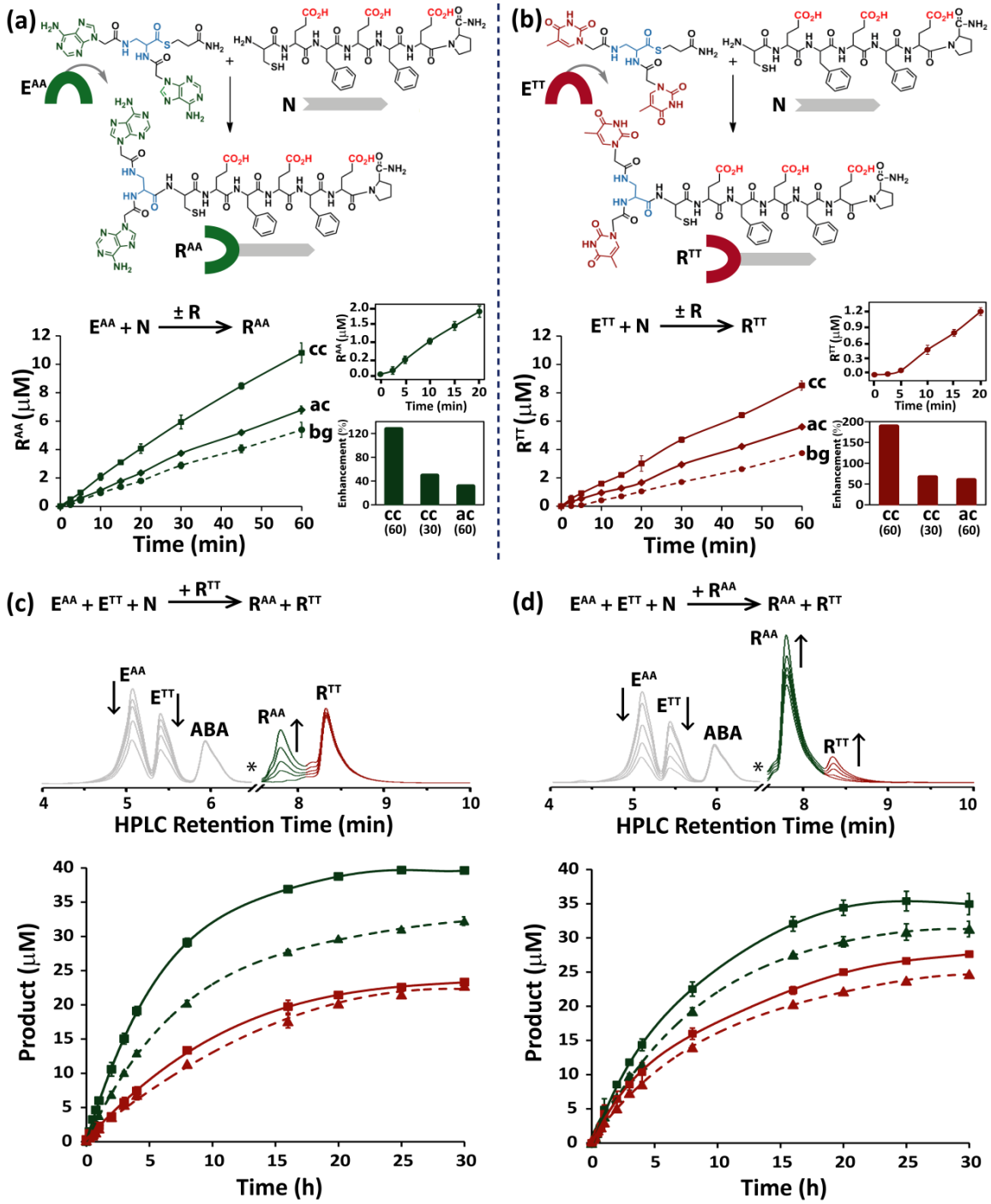

Figure 1. Nucleopeptide replication networks. a,b) Native chemical ligation reactions forming the $\mathbf{R}^{AA}$ and $\mathbf{R}^{TT}$ conjugates from their respective electrophile and nucleophile precursors (at pH 7.4 the Glu side chain carboxylic acids would be in their deprotonated anionic form), and time-dependent formation of these conjugates in template-free (bg), autocatalytic (ac), and cross-catalytic (cc) reactions. Reactions were carried out with 100 μM $\mathbf{E}^{AA}$ or $\mathbf{E}^{TT}$ and 100 μM **N**, either in the absence of a template (bg) or when seeded with the designated amount of template at initiation (ac/cc). Insets show the early stages of the background reactions, highlighting the lag phase typical of product formation through autocatalysis (*top insets*), and the rate enhancement (%) in cross-catalytic reactions seeded with 60 μM or 30 μM of template or in autocatalytic reactions seeded with 60 μM template (*bottom insets*). (c,d) Time-dependent analysis of the replicator-assisted product formation of the conjugates $\mathbf{R}^{AA}$ (*green*) and $\mathbf{R}^{TT}$ (*red*) in network reactions initiated with

$\mathbf{E}^{\mathbf{AA}}$ (50 μM), $\mathbf{E}^{\mathbf{TT}}$ (50 μM) and **N** (100 μM), and seeded with 20 μM (dashed lines) or 60 μM (solid lines) of $\mathbf{R}^{\mathbf{TT}}$ (c) or $\mathbf{R}^{\mathbf{AA}}$ (d). HPLC chromatograms (*top*) indicate the increase in $\mathbf{R}^{\mathbf{AA}}$ and $\mathbf{R}^{\mathbf{TT}}$ product over time in representative reactions seeded with 60 μM $\mathbf{R}^{\mathbf{TT}}$ (c) or 60 μM $\mathbf{R}^{\mathbf{AA}}$ (d); Note that $\mathbf{R}^{\mathbf{TT}}$ and $\mathbf{R}^{\mathbf{AA}}$ peaks have initial intensity due to seeding (in (c) and (d), respectively), and that the * symbols denote minor (≥ 15%) branched product peaks, removed for clarity (see also Fig. s20). All reactions were carried out in duplicate, in HEPES buffer, pH 7.4, in the presence of TCEP as a reducing agent (5 mM) and with 4-acetamido benzoic acid (ABA; 30 μM) as the internal standard. Data were acquired by HPLC analysis of aliquots collected at the designated times (Figs. s17-s20).

As subtle changes in the sequence or assembly conditions of NA–pep conjugates can lead to the formation of significantly different supramolecular architectures,[5,6] the assembly structures of the replicators $\mathbf{R}^{\mathbf{AA}}$ and $\mathbf{R}^{\mathbf{TT}}$ (60 μM) – in separate solutions or when mixed together – were subsequently studied in a set of microscopy and spectroscopy assays (Fig. 2). Atomic force microscopy (AFM) and transmission electron microscopy (TEM) images of $\mathbf{R}^{\mathbf{AA}}$ revealed (bundled) fiber architectures, 7–8 nm wide and up to a few microns long (Fig. 2a). In contrast, images of $\mathbf{R}^{\mathbf{TT}}$ showed small (diameter ≤ 15 nm) spherical aggregates (Fig. 2b). Staining of the two types of assembly with thioflavin T (ThT) and emission analysis using ensemble fluorescence spectroscopy (Fig. 2d,e) and confocal microscopy (Fig. 2a,b – *right-hand panels*) revealed β-sheet-rich domains and stacked nucleobases. Significant characteristic emission was observed for the stained $\mathbf{R}^{\mathbf{AA}}$ fibers, but only weak emission signals were detected after staining the $\mathbf{R}^{\mathbf{TT}}$ spherical assemblies, thus further underlining the substantial differences between the molecular arrangements within the two aggregates. Interestingly, the AFM, TEM and fluorescence microscopy images obtained for equimolar mixtures of $\mathbf{R}^{\mathbf{AA}}$ and $\mathbf{R}^{\mathbf{TT}}$ ($\mathbf{R}^{\mathbf{AA}}$:$\mathbf{R}^{\mathbf{TT}}$; 30 μM each) showed yet another morphology, in which more condensed matter at the center of the assembly was contained within an environment of lower density aggregates, presumably liquid droplets with diameters ranging roughly from 35 nm to 75 nm (Fig. 2c and Fig. s22). We then performed fluorescence recovery after photobleaching (FRAP) experiments to determine the diffusion kinetics of ThT in and out of these liquid droplets. Individual droplets were photobleached and imaged for fluorescence recovery over 30 seconds (Fig. 2c), while other (control) droplets were imaged without bleaching (Fig. s22f). Significant recovery of fluorescence indicated the propensity of the droplet-like assemblies to allow in/out ThT diffusion, confirming their formation through liquid-liquid phase separation processes, similarly to other synthetic and cellular aggregates.[50]

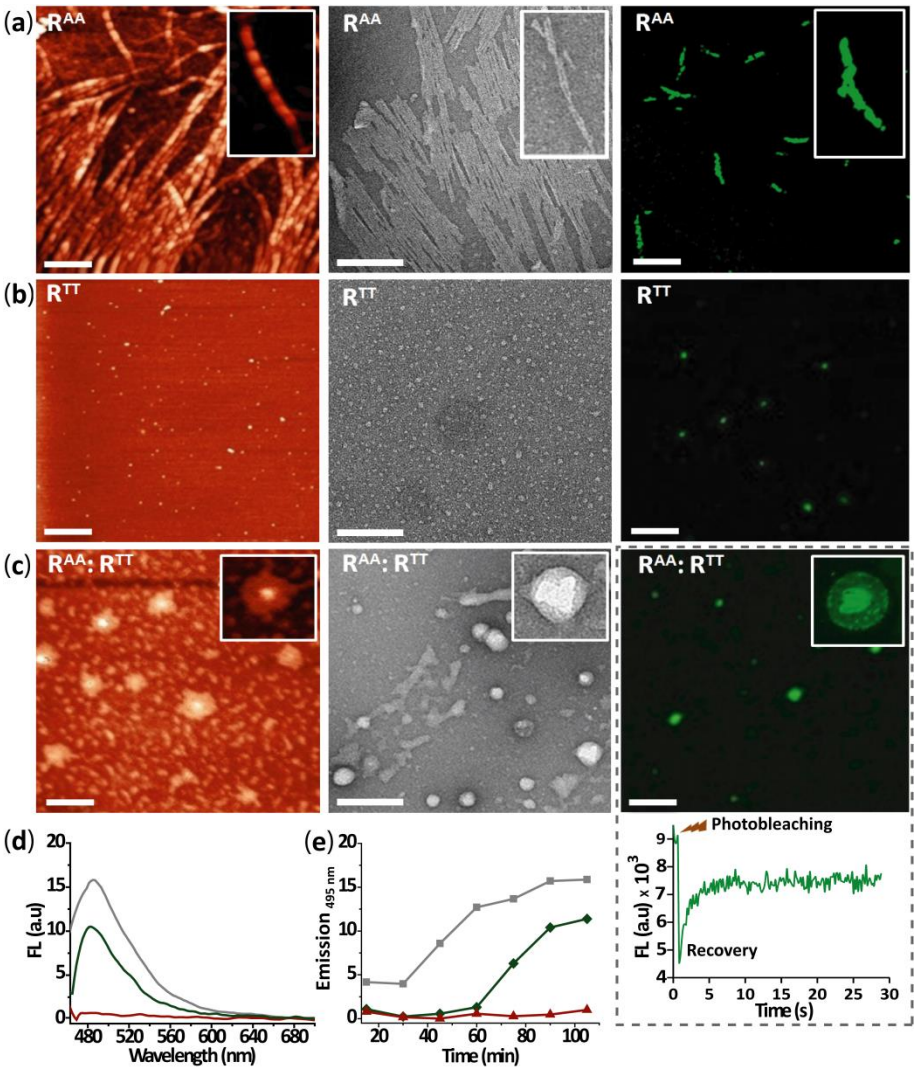

Figure 2. $\mathbf{R^{AA}}$ and $\mathbf{R^{TT}}$ self-assembled nanostructures. a-c) AFM (*left*), TEM (*middle*) and fluorescence microscopy (*right*) images obtained for assemblies of 60 μM $\mathbf{R^{AA}}$, 60 μM $\mathbf{R^{TT}}$ and equimolar (30 μM each) mixtures of $\mathbf{R^{AA}}$ and $\mathbf{R^{TT}}$ ($\mathbf{R^{AA}}$:$\mathbf{R^{TT}}$). Scale bars: AFM 500 nm; TEM 200 nm; fluorescence microscopy 10 μm. TEM samples were stained with uranyl acetate, and fluorescence microscopy samples with thioflavin T (ThT). Inset in the right-hand side of panel (c) shows the fluorescence recovery after ThT photobleaching (FRAP) in the liquid droplets. (d) Emission spectra observed following ThT binding to $\mathbf{R^{AA}}$ (—), $\mathbf{R^{TT}}$ (—) and $\mathbf{R^{AA}}$:$\mathbf{R^{TT}}$ (—). (e) Kinetics of ThT binding to $\mathbf{R^{AA}}$ (♦), $\mathbf{R^{TT}}$ (▲) and $\mathbf{R^{AA}}$:$\mathbf{R^{TT}}$ (■). Experiments were performed in buffer (pH 7.4) at room temperature.

The kinetics of product formation in the individual replication reactions and within the small networks (Fig. 1), taken together with the structural information obtained for $\mathbf{R^{AA}}$ and $\mathbf{R^{TT}}$ assemblies (Fig. 2), allowed us to draw up the asymmetric network topology that selectively yields higher amounts of $\mathbf{R^{AA}}$ versus $\mathbf{R^{TT}}$ (Fig. 3a). Based on previous studies with assembly-dependent replication systems,[46,51] we expected the newly formed spheres and fibers to be the dominant catalytic entities. These assemblies can facilitate association of the precursor molecules at the assembly edges or points

of imperfection, and consequently enhance their ligation. The network asymmetry emerges because while both $\mathbf{R}^{\mathbf{AA}}$ and $\mathbf{R}^{\mathbf{TT}}$ form via cross-catalysis – templated by spheres and fibers, respectively – $\mathbf{R}^{\mathbf{AA}}$ also replicates in a 'selfish' autocatalytic pathway enhanced by the fibers. Moreover, the cross-catalytic pathway leading to the formation of $\mathbf{R}^{\mathbf{AA}}$ is more efficient than the reciprocal pathway forming $\mathbf{R}^{\mathbf{TT}}$ (Fig. 1c,d). Based on this network topology, we constructed a kinetic model representing the multiple active reaction steps: 1) assembly of $\mathbf{R}^{\mathbf{AA}}$ and $\mathbf{R}^{\mathbf{TT}}$ into catalytic species, and their spontaneous disassembly into smaller aggregates featuring higher number of catalytic edges;[52] 2) background ligations; 3) template-assisted autocatalysis; and 4) template-assisted cross-catalytic reactions (Fig. 3b). This model enabled us to probe the product formation profiles in multiple scenarios simply by manipulating the relevant kinetic constants and/or initial conditions.

We ran an elaborate simulation in Matlab (Supplementary methods S7),[45,52] starting with a set of initial concentrations that directly matched the experimental conditions. The template-assisted kinetic constants reflected the observed order of catalytic activity by assigning $b^{AT} > b^{AA} \sim b^{TA} > b^{TT}$, while other parameters were applied based on experimental data and/or previous simulations of related systems (e.g., fibril-dependent peptide replication[45]), and were grouped together to simplify the analysis when possible (Supplementary Table s1). The results of this simple modeling under 'native' conditions (Fig. 3c,d and Figs. s24 and s25) closely reproduced the replication kinetic profiles observed experimentally for both individual reactions and small networks (Fig. 1). In particular, the selectivity product ratio (Pr = $\mathbf{R}^{\mathbf{AA}}/\mathbf{R}^{\mathbf{TT}}$) in the simulated network (see Fig. 3c) nicely matched the experimentally observed ratio. We then applied the simulation analysis to screen for the network growth kinetics that would have been obtained had the network been governed by a different set of interactions. This exercise allowed us to display network behavior that would otherwise have been difficult to predict and thereby to guide the design of new experiments in which the selectivity towards one of the replicators would be further enhanced (see below). Consequently, imposing more stringent competition conditions through initiation of the reactions with an under-stoichiometric amount of **N** ($[\mathbf{E}^{\mathbf{AA}}] = [\mathbf{E}^{\mathbf{TT}}] = [\mathbf{N}] = 67$ μM) led to a higher P_r values (Fig. 3e,f). Studying the network when the template-free background reactions were allegedly slower than in the 'native' cases, simply applied by lowering the g^A and g^T values (Fig. 3b) by one order of magnitude, revealed the higher inherent selectivity of the template-assisted processes towards the production of $\mathbf{R}^{\mathbf{AA}}$ (Fig. 3g,h). Finally, simulating the network for cases in which the assembly seed of one of the supramolecular structures – spheres (Fig. 3i and Fig. s28) or fibers (Fig. 3j and Fig. s29) – becomes active in a lower aggregation state than the other (achieved by manipulating the minimum seed assembly value m; Table s1) also dramatically affected the competition, yielding high P_r values towards the selection of $\mathbf{R}^{\mathbf{AA}}$ (Fig. 3i,j).

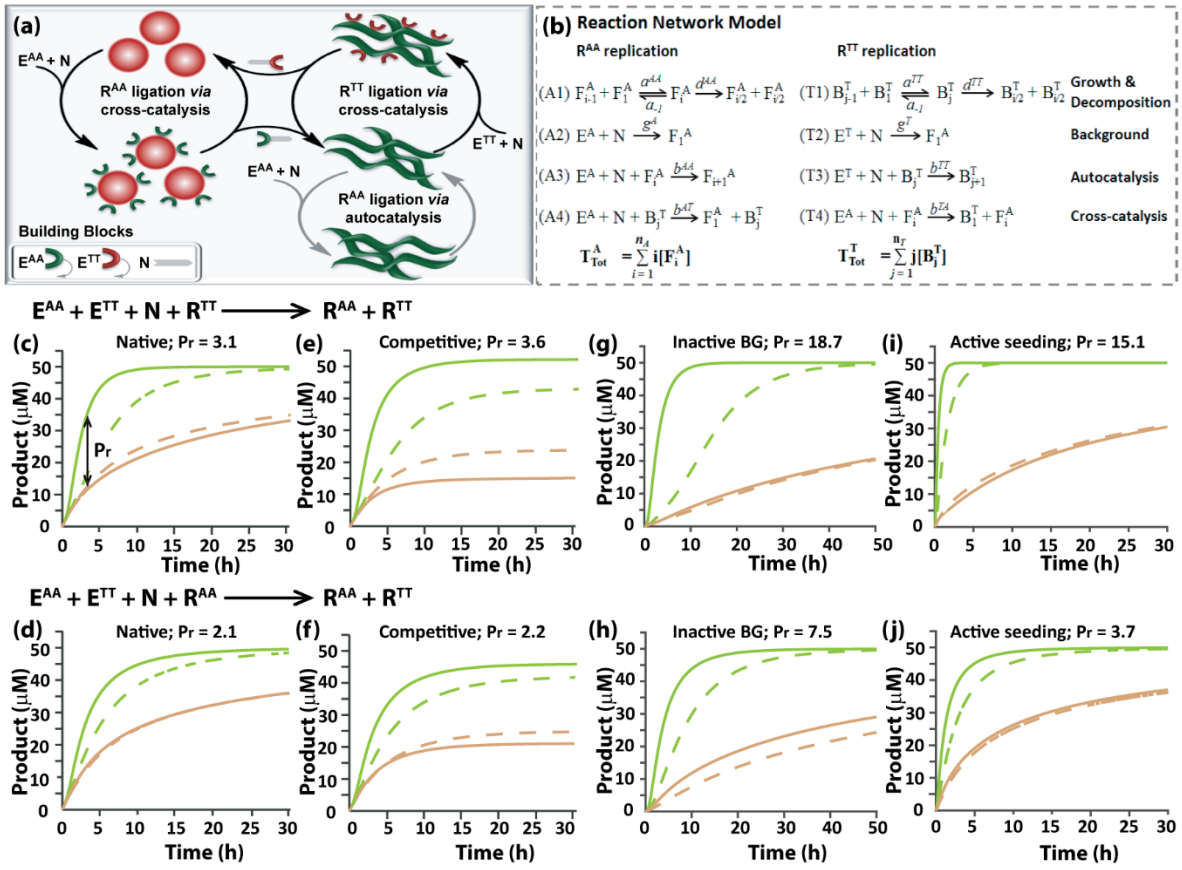

Figure 3. Simulation analysis of selective product formation within binary nucleopeptide networks. (a) Schematic representation of the network topology and operative catalytic pathways. (b) Reaction model describing the multiple simultaneous processes taking place in the network. F and B type species refer to the growing fibers and spheres, respectively, and kinetic constants are described in the SI Section S7 and Table s1. (c-j) Time-dependent simulation results obtained on the basis of the reaction network model in (b) and by applying variable initial conditions and/or kinetic constants corresponding to real and putative experimental scenarios (Table s1). Simulation results in the upper row (panels c, e, g, i) and lower row (d, f, h, j) were obtained for network reactions seeded with $\mathbf{R}^{\mathbf{TT}}$ and $\mathbf{R}^{\mathbf{AA}}$, respectively. In all cases, the production of $\mathbf{R}^{\mathbf{AA}}$ and $\mathbf{R}^{\mathbf{TT}}$ is shown in green and brown-red, respectively; product formation in a reaction seeded with 20 μM or 60 μM of the template is shown in dashed and solid lines, respectively. Native: $[\mathbf{E}^{\mathbf{AA}}] = [\mathbf{E}^{\mathbf{TT}}] =$ 50 μM; $[\mathbf{N}] =$ 100 μM. Competitive: $[\mathbf{E}^{\mathbf{AA}}] = [\mathbf{E}^{\mathbf{TT}}] = [\mathbf{N}] =$ 67 μM. Inactive background (BG): same initial conditions as "Native" but with significantly weaker background reactions (g = 0.1). Active seeding: same initial conditions and rate constants as "Native", but with enhanced or reduced seeding (m_A or m_T set at 5 and/or 25, instead of 10). Pr values, reflecting the $\mathbf{R}^{\mathbf{AA}}$ to $\mathbf{R}^{\mathbf{TT}}$ selectivity ratios, are added at the title of each panel; these were calculated for the 60 μM seeded reactions, where the ratios between $\mathbf{R}^{\mathbf{AA}}$ and $\mathbf{R}^{\mathbf{TT}}$ were maximal, as indicated for example by the double-headed arrow inserted in panel c.

The selection pressure within networks of coexisting replicators can be intensified under conditions of constant flow, in which the catalytic pathways are kept far from equilibrium (Fig. 4).[53] Production of the $\mathbf{R}^{\mathbf{AA}}$ and $\mathbf{R}^{\mathbf{TT}}$ replicators in competition experiments was therefore studied over a few hours in a small-volume continuously stirred tank reactor (CSTR; Fig. 4a). The first sets of experiments were conducted with either stoichiometric (total) amounts of the electrophiles $\mathbf{E}^{\mathbf{AA}}$ and $\mathbf{E}^{\mathbf{TT}}$ versus the nucleophile **N** (1:1:2), similarly to the batch reaction experiments (Fig. 1c,d), or with equal molar

amounts of $\mathbf{E}^{\mathbf{AA}}$, $\mathbf{E}^{\mathbf{TT}}$ and **N** (1:1:1), thereby imposing stringent competition and potentially enhanced selectivity (Fig. 3e,f). For each experiment, we studied the background reaction and 20 μM $\mathbf{R}^{\mathbf{TT}}$-seeded or 20 μM $\mathbf{R}^{\mathbf{AA}}$-seeded reactions. The background experiments revealed more pronounced selectivity towards the formation of $\mathbf{R}^{\mathbf{AA}}$ in comparison with the selectivity observed in the batch reactions, and the selectivity ratio was indeed further enhanced under the conditions of stringent competition (Fig. 4b,c&f). Most dramatically, the seeded reactions (in either the 1:1:2 or 1:1:1 initial concentration ratios) yielded much higher formation of $\mathbf{R}^{\mathbf{AA}}$ than $\mathbf{R}^{\mathbf{TT}}$ (Figs. s30 and s31, and Fig. 4d-f), revealing a selectivity higher by more than one order of magnitude at steady state for the 1:1:1 case.

To further tune selective product formation by nucleic-acid-related recognition processes, nucleobase analogs, namely, 2-aminopurine (2-AP) as an adenine analog and 5-bromouracil (5-BU) as a thymine analog,[54,55] were added to the replicator-seeded reactions. Each of these aromatic bases can primarily hybridize with the conjugate-containing complementary bases (i.e., 2-AP with $\mathbf{R}^{\mathbf{TT}}$ and 5-BU with $\mathbf{R}^{\mathbf{AA}}$; see hybridization motifs in Scheme s1c) and consequently non-covalently inhibit the template-assisted reaction pathways originated by the latter. As a result of inhibition by 2-AP in the $\mathbf{R}^{\mathbf{TT}}$-seeded reaction, we observed lower selectivity due to a decrease in $\mathbf{R}^{\mathbf{AA}}$ formation, accompanied by an increase in the production of $\mathbf{R}^{\mathbf{TT}}$ (Fig. 4d). Alternatively, inhibition by 5-BU in the $\mathbf{R}^{\mathbf{AA}}$-seeded reaction resulted in higher formation of $\mathbf{R}^{\mathbf{AA}}$, leading to pronounced selectivity (Pr ~ 5), since $\mathbf{R}^{\mathbf{TT}}$ formation remained almost unchanged (Fig. 4e). If higher-than-stoichiometric amounts of 5-BU were added to the $\mathbf{R}^{\mathbf{AA}}$-seeded reaction, the selectivity towards $\mathbf{R}^{\mathbf{AA}}$ formation did not change greatly, probably due to inhibition of additional catalytic pathways in the network.

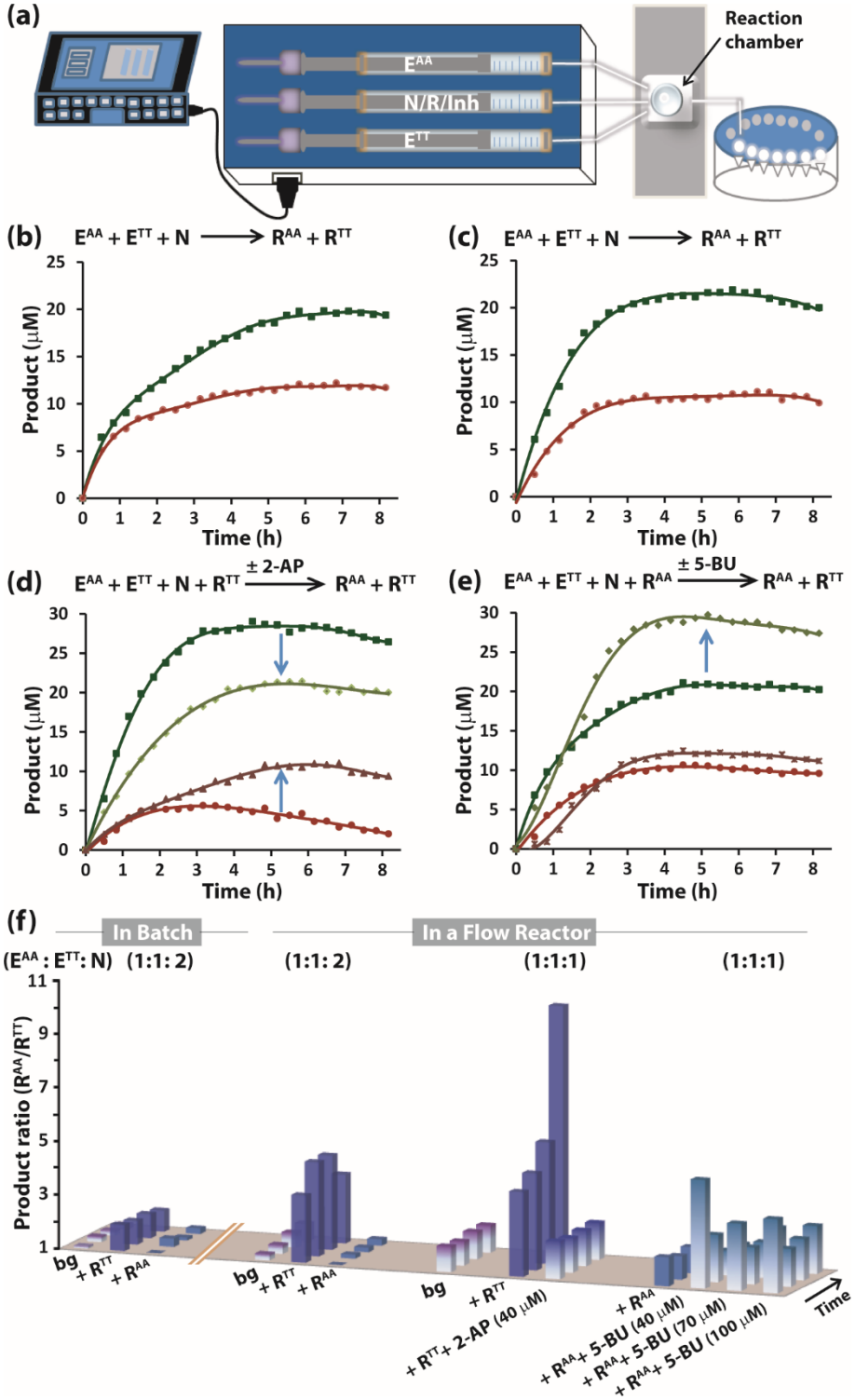

Figure 4. Selective product formation far from equilibrium. (a) Schematic illustration of the continuously stirred tank reactor. (b,c) Time-dependent product formation in the background reactions, where $\mathbf{E}^{\mathbf{AA}}$:$\mathbf{E}^{\mathbf{TT}}$:**N** = 1:1:2 (b) and $\mathbf{E}^{\mathbf{AA}}$:$\mathbf{E}^{\mathbf{TT}}$:**N** = 1:1:1 (c). (d) Time-dependent product formation in the $\mathbf{R}^{\mathbf{TT}}$-assisted reactions ($\mathbf{E}^{\mathbf{AA}}$:$\mathbf{E}^{\mathbf{TT}}$:**N** = 1:1:1) in the absence or presence of 40 μM 2-AP. (e) Time-dependent product formation in the $\mathbf{R}^{\mathbf{AA}}$-assisted reactions ($\mathbf{E}^{\mathbf{AA}}$:$\mathbf{E}^{\mathbf{TT}}$:**N** = 1:1:1) in the absence or presence of 40 μM 5-BU. (f) Comparison of the product ratio ($\mathbf{R}^{\mathbf{AA}}$/$\mathbf{R}^{\mathbf{TT}}$) over time for a large set of experiments carried out in batch mode and under flow conditions. All reactions were carried out in HEPES buffer pH 7.4, at room temperature.

In summary, we have shown that pronounced selectivity towards the production of one nucleopeptide over another in small, plausibly prebiotic, networks can result from the synergistic activity between a nucleobase domain, delivering inter-conjugate hybridization, and a peptide domain, which stabilizes different assembly architectures. We hold that this study is significantly relevant to the search for the "origin-of-life molecules"—those potentially prebiotic small molecules and proto-polymers that, through self-organization, could facilitate the transition from nonliving matter to the first primitive life. Recent publications have indicated that peptide and nucleic acid precursors could be formed in a prebiotic environment through common synthetic routes,[56,57] and they thus support our proposition that synergistic activity developed at a later stage may have led to the selection of functional chimeras. Other recent studies have confirmed synergy in NA–pep systems, affording, for example, peptide formation on short RNA or ribozymes,[58-60] enantio-selective RNA precursor synthesis by amino acids,[61] peptide nucleic acid (PNA)-templated replication,[62] and more.[63] Since our study highlights the effect of synergistic interactions both on the thermodynamics of the hybrid systems, leading to the formation of different assembly structures, and on the kinetics of template-directed replication processes, it may explain the rapid progression in complexity of systems chemistry in primitive environments, which would have facilitated the development of a large repertoire of functions.

Acknowledgements

We thank Prof. D.G. Lynn (Emory University) for fruitful discussions. The research was supported by the H2020 FET-Open (A.d.l.E and G.A.; CLASSY project, Grant Agreement Nº 862081), an NSF-BSF grant (GA; BSF-2015671), and the Spanish Ministry of Economy and Competitivity (A.d.l.E; MINECO: CTQ-2014-53673-P, CTQ-2017-89539-P, and EUIN2017-87022). The European COST Action CM1304 funded a Short-Term Scientific Mission of S.M.R. to BGU. A.K.B. received support from the BGU Kreitmann fellowships program.

Authors contribution

A.K.B, A.d.l.E. and G.A. conceived the study. A.K.B., H.S., S.M.-R., A.C.-O. and K.B. designed and performed the experiments. N.W. performed the kinetic simulation analyses. A.K.B, and G.A. co-wrote the paper, and all the authors discussed the results and commented on the paper.

References

1. Sanbonmatsu, K. Y. Large-scale simulations of nucleoprotein complexes: ribosomes, nucleosomes, chromatin, chromosomes and CRISPR. *Curr. Opin. Struct. Biol.* **55**, 104-113, (2019).
2. Yonath, A. Polar Bears, antibiotics, and the evolving ribosome (Nobel Lecture). *Angew. Chem., Int. Ed.* **49**, 4340-4354, (2010).
3. Perlmutter, J. D. & Hagan, M. F. Mechanisms of virus assembly. *Annu. Rev. Phys. Chem.* **66**, 217-239, (2015).
4. Bowman, J. C., Petrov, A. S., Frenkel-Pinter, M., Penev, P. I. & Williams, L. D. Root of the tree: the significance, evolution, and origins of the ribosome. *Chem. Rev.* **120**, 4848-4878, (2020).
5. Freeman, R., Han, M., Alvarez, Z., Lewis, J. A., Wester, J. R., Stephanopoulos, N., McClendon, M. T., Lynsky, C., Godbe, J. M., Sangji, H., Luijten, E. & Stupp, S. I. Reversible self-assembly of superstructured networks. *Science* **362**, 808-813, (2018).
6. Chotera, A., Sadihov, H., Cohen-Luria, R., Monnard, P.-A. & Ashkenasy, G. Functional assemblies emerging in complex mixtures of peptides and nucleic acid-peptide chimeras. *Chem. Eur. J.* **24**, 10128-10135, (2018).
7. Rha, A. K., Das, D., Taran, O., Ke, Y., Mehta, A. K. & Lynn, D. G. Electrostatic complementarity drives amyloid/nucleic acid co-assembly. *Angew. Chem., Int. Ed.* **59**, 358-363, (2020).
8. Jiang, T., Meyer, T. A., Modlin, C., Zuo, X., Conticello, V. P. & Ke, Y. Structurally ordered nanowire formation from co-assembly of DNA origami and collagen-mimetic peptides. *J. Am. Chem. Soc.* **139**, 14025-14028, (2017).
9. Liu, B., Pappas, C. G., Zangrando, E., Demitri, N., Chmielewski, P. J. & Otto, S. Complex molecules that fold like proteins can emerge spontaneously. *J. Am. Chem. Soc.* **141**, 1685-1689, (2019).
10. Ni, R. & Chau, Y. Tuning the inter-nanofibril interaction to regulate the morphology and function of peptide/DNA co-assembled viral mimics. *Angew. Chem., Int. Ed.* **56**, 9356-9360, (2017).
11. Buchberger, A., Simmons, C. R., Fahmi, N. E., Freeman, R. & Stephanopoulos, N. Hierarchical assembly of nucleic acid/coiled-coil peptide nanostructures. *J. Am. Chem. Soc.* **142**, 1406-1416, (2020).
12. Humenik, M. & Scheibel, T. Nanomaterial building blocks based on spider silk-oligonucleotide conjugates. *ACS Nano* **8**, 1342-1349, (2014).
13. Raymond, D. M. & Nilsson, B. L. Multicomponent peptide assemblies. *Chem. Soc. Rev.* **47**, 3659-3720, (2018).
14. Stephanopoulos, N. Peptide-oligonucleotide hybrid molecules for bioactive nanomaterials. *Bioconjugate Chemistry* **30**, 1915-1922, (2019).
15. Toste, F. D., Sigman, M. S. & Miller, S. J. Pursuit of noncovalent interactions for strategic site-selective catalysis. *Acc. Chem. Res.* **50**, 609-615, (2017).
16. Korendovych, I. V. & DeGrado, W. F. Catalytic efficiency of designed catalytic proteins. *Curr. Opin. Struct. Biol.* **27**, 113-121, (2014).
17. Zozulia, O., Dolan, M. A. & Korendovych, I. V. Catalytic peptide assemblies. *Chem. Soc. Rev.* **47**, 3621-3639, (2018).
18. Goodwin, J. T., Mehta, A. K. & Lynn, D. G. Digital and analog chemical evolution. *Acc. Chem. Res.* **45**, 2189-2199, (2012).
19. Bai, Y., Chotera, A., Taran, O., Liang, C., Ashkenasy, G. & Lynn, D. G. Achieving biopolymer synergy in systems chemistry. *Chem. Soc. Rev.* **47**, 5444-5456, (2018).
20. Frenkel-Pinter, M., Samanta, M., Ashkenasy, G. & Leman, L. J. Prebiotic peptides: molecular hubs in the Origin of Life. *Chem. Rev.* **120**, 4707-4765, (2020).

21. Gibard, C., Bhowmik, S., Karki, M., Kim, E.-K. & Krishnamurthy, R. Phosphorylation, oligomerization and self-assembly in water under potential prebiotic conditions. *Nat. Chem.* **10**, 212-217, (2018).
22. Morales-Reina, S., Giri, C., Leclercq, M., Vela-Gallego, S., de la Torre, I., Castón, J. R., Surin, M. & de la Escosura, A. Programmed recognition between complementary dinucleolipids to control the self-assembly of lipidic amphiphiles. *Chem. Eur. J.* **26**, 1082-1090, (2020).
23. Bonfio, C., Godino, E., Corsini, M., Fabrizi de Biani, F., Guella, G. & Mansy, S. S. Prebiotic iron-sulfur peptide catalysts generate a pH gradient across model membranes of late protocells. *Nat. Catal.* **1**, 616-623, (2018).
24. Forsythe, J. G., Yu, S.-S., Mamajanov, I., Grover, M. A., Krishnamurthy, R., Fernandez, F. M. & Hud, N. V. Ester-mediated amide bond formation driven by wet-dry cycles: a possible path to polypeptides on the prebiotic Earth. *Angew. Chem. Int. Ed.* **54**, 9871-9875, (2015).
25. Eigen, M. & Schuster, P. *The hypercycle. A principle of natural self-organization.*, (Springer, 1979).
26. Kauffman, S. A. Autocatalytic sets of proteins. *J. Theor. Biol.* **119**, 1-24, (1986).
27. Matsumura, S., Kun, Á., Ryckelynck, M., Coldren, F., Szilágyi, A., Jossinet, F., Rick, C., Nghe, P., Szathmáry, E. & Griffiths, A. D. Transient compartmentalization of RNA replicators prevents extinction due to parasites. *Science* **354**, 1293-1296, (2016).
28. O'Flaherty, D. K., Kamat, N. P., Mirza, F. N., Li, L., Prywes, N. & Szostak, J. W. Copying of mixed-sequence RNA templates inside model protocells. *J. Am. Chem. Soc.* **140**, 5171-5178, (2018).
29. Semenov, S. N., Wong, A. S. Y., van der Made, R. M., Postma, S. G. J., Groen, J., van Roekel, H. W. H., de Greef, T. F. A. & Huck, W. T. S. Rational design of functional and tunable oscillating enzymatic networks. *Nat. Chem.* **7**, 160-165, (2015).
30. Maity, I., Wagner, N., Mukherjee, R., Dev, D., Peacock-Lopez, E., Cohen-Luria, R. & Ashkenasy, G. A chemically fueled non-enzymatic bistable network. *Nature Communications* **10**, 4636, (2019).
31. Semenov, S. N., Kraft, L. J., Ainla, A., Zhao, M., Baghbanzadeh, M., Campbell, V. E., Kang, K., Fox, J. M. & Whitesides, G. M. Autocatalytic, bistable, oscillatory networks of biologically relevant organic reactions. *Nature* **537**, 656-660, (2016).
32. Cafferty, B. J., Wong, A. S. Y., Semenov, S. N., Belding, L., Gmur, S., Huck, W. T. S. & Whitesides, G. M. Robustness, entrainment, and hybridization in dissipative molecular networks, and the Origin of Life. *J. Am. Chem. Soc.* **141**, 8289-8295, (2019).
33. Huck, J., Kosikova, T. & Philp, D. Compositional persistence in a multicyclic network of synthetic replicators. *J. Am. Chem. Soc.* **141**, 13905-13913, (2019).
34. He, M. & Lehn, J.-M. Time-Dependent Switching of Constitutional Dynamic Libraries and Networks from Kinetic to Thermodynamic Distributions. *J. Am. Chem. Soc.* **141**, 18560-18569, (2019).
35. Zhou, Z., Yue, L., Wang, S., Lehn, J.-M. & Willner, I. DNA-Based Multiconstituent Dynamic Networks: Hierarchical Adaptive Control over the Composition and Cooperative Catalytic Functions of the Systems. *J. Am. Chem. Soc.* **140**, 12077-12089, (2018).
36. Wagner, N., Alasibi, S., Peacock-Lopez, E. & Ashkenasy, G. Coupled oscillations and circadian rhythms in molecular replication networks. *J. Phys. Chem. Lett.* **6**, 60-65, (2015).
37. Ruiz-Mirazo, K., Briones, C. & de la Escosura, A. Prebiotic systems chemistry: new perspectives for the Origins of Life. *Chem. Rev.* **114**, 285-366, (2014).
38. Kosikova, T. & Philp, D. Exploring the emergence of complexity using synthetic replicators. *Chem. Soc. Rev.* **46**, 7274-7305, (2017).
39. Bissette, A. J. & Fletcher, S. P. Mechanisms of autocatalysis. *Angew. Chem. Int. Ed.* **52**, 12800-12826, (2013).
40. Ruiz-Mirazo, K., Briones, C. & de la Escosura, A. Chemical roots of biological evolution: the origins of life as a process of development of autonomous functional systems. *Open. Biol.* **7**, (2017).

41. Huang, L., Krupkin, M., Bashan, A., Yonath, A. & Massa, L. Protoribosome by quantum kernel energy method. *Proc. Natl. Acad. Sci. USA* **110**, 14900-14905, (2013).
42. Li, J., Nowak, P. & Otto, S. Dynamic combinatorial libraries: from exploring molecular recognition to Systems Chemistry. *J. Am. Chem. Soc.* **135**, 9222-9239, (2013).
43. Dadon, Z., Wagner, N. & Ashkenasy, G. The road to non-enzymatic molecular networks. *Angew. Chem. Int. Ed.* **47**, 6128-6136, (2008).
44. Sadownik, J. W., Mattia, E., Nowak, P. & Otto, S. Diversification of self-replicating molecules. *Nat. Chem.* **8**, 264-269, (2016).
45. Nanda, J., Rubinov, B., Ivnitski, D., Mukherjee, R., Shtelman, E., Motro, Y., Miller, Y., Wagner, N., Cohen-Luria, R., Ashkenasy, G. & Nanda, J. Emergence of native peptide sequences in prebiotic replication networks. *Nature Communications* **8**, 434, (2017).
46. Colomer, I., Borissov, A. & Fletcher, S. P. Selection from a pool of self-assembling lipid replicators. *Nature Communications* **11**, 176, (2020).
47. Kosikova, T. & Philp, D. Two synthetic replicators compete to process a dynamic reagent pool. *J. Am. Chem. Soc.* **141**, 3059-3072, (2019).
48. Liu, B., Pappas, C. G., Ottele, J., Schaeffer, G., Jurissek, C., Pieters, P. F., Altay, M., Maric, I., Stuart, M. C. A. & Otto, S. Spontaneous emergence of self-replicating molecules containing nucleobases and amino acids. *J. Am. Chem. Soc.* **142**, 4184-4192, (2020).
49. Ashkenasy, G., Hermans, T. M., Otto, S. & Taylor, A. F. Systems chemistry. *Chem. Soc. Rev.* **46**, 2543-2554, (2017).
50. Aumiller, W. M., Jr. & Keating, C. D. Phosphorylation-mediated RNA/peptide complex coacervation as a model for intracellular liquid organelles. *Nat. Chem.* **8**, 129-137, (2016).
51. Rubinov, B., Wagner, N., Rapaport, H. & Ashkenasy, G. Self-Replicating Amphiphilic β-Sheet Peptides. *Angew. Chem. Int. Ed.* **48**, 6683-6686, (2009).
52. Rubinov, B., Wagner, N., Matmor, M., Regev, O., Ashkenasy, N. & Ashkenasy, G. Transient fibril structures facilitating non-enzymatic self-replication. *ACS nano* **6**, 7893-7901, (2012).
53. Szathmary, E. & Gladkih, I. Subexponential growth and coexistence of nonenzymically replicating templates. *J. Theor. Biol.* **138**, 55-58, (1989).
54. Watanabe, S. M. & Goodman, M. F. Kinetic measurement of 2-aminopurine·cytosine and 2-aminopurine·thymine base pairs as a test of DNA polymerase fidelity mechanisms. *Proc. Natl. Acad. Sci. U. S. A.* **79**, 6429-6433, (1982).
55. Fazakerley, G. V., Sowers, L. C., Eritja, R., Kaplan, B. E. & Goodman, M. F. Structural and dynamic properties of a bromouracil-adenine base pair in DNA studied by proton NMR. *J. Biomol. Struct. Dyn.* **5**, 639-650, (1987).
56. Patel, B. H., Percivalle, C., Ritson, D. J., Duffy, C. D. & Sutherland, J. D. Common origins of RNA, protein and lipid precursors in a cyanosulfidic protometabolism. *Nat. Chem.* **7**, 301–307, (2015).
57. Islam, S., Bucar, D.-K. & Powner, M. W. Prebiotic selection and assembly of proteinogenic amino acids and natural nucleotides from complex mixtures. *Nat. Chem.* **9**, 584-589, (2017).
58. Turk, R. M., Illangasekare, M. & Yarus, M. Catalyzed and Spontaneous Reactions on Ribozyme Ribose. *J. Am. Chem. Soc.* **133**, 6044-6050, (2011).
59. Griesser, H., Bechthold, M., Tremmel, P., Kervio, E. & Richert, C. Amino acid-Specific, ribonucleotide-promoted peptide formation in the absence of enzymes. *Angew. Chem., Int. Ed.* **56**, 1224-1228, (2017).
60. Griesser, H., Tremmel, P., Kervio, E., Pfeffer, C., Steiner, U. E. & Richert, C. Ribonucleotides and RNA promote peptide chain growth. *Angew. Chem., Int. Ed.* **56**, 1219-1223, (2017).
61. Hein, J. E., Tse, E. & Blackmond, D. G. A route to enantiopure RNA precursors from nearly racemic starting materials. *Nat. Chem.* **3**, 704-706, (2011).
62. Ura, Y., Beierle, J. M., Leman, L. J., Orgel, L. E. & Ghadiri, M. R. Self-assembling sequence-adaptive peptide nucleic acids. *Science* **325**, 73-77, (2009).

63. Frenkel-Pinter, M., Haynes, J. W., Mohyeldin, A. M., C, M., Sargon, A. B., Petrov, A. S., Krishnamurthy, R., Hud, N. V., Williams, L. D. & Leman, L. J. Mutually stabilizing interactions between proto-peptides and RNA. *Nature Communications* **11**, 3137, (2020).